



## OPEN ACCESS

## EDITED BY

Bing Bai,  
Beijing Jiaotong University, China

## REVIEWED BY

Pan Liu,  
Guangzhou Maritime College, China  
Ming Zhang,  
Zhengzhou University of Aeronautics,  
China

## \*CORRESPONDENCE

Xue qiang Yang,  
✉ xqyfs@126.com

RECEIVED 29 August 2023

ACCEPTED 04 October 2023

PUBLISHED 03 November 2023

## CITATION

Deng X, Zhu Z, Lin Xy and Yang Xq (2023),  
Effect of matrix suction on the shear  
strength characteristics of reinforced  
granite residual soil.  
*Front. Mater.* 10:1284722.  
doi: 10.3389/fmats.2023.1284722

## COPYRIGHT

© 2023 Deng, Zhu, Lin and Yang. This is  
an open-access article distributed under  
the terms of the [Creative Commons  
Attribution License \(CC BY\)](#). The use,  
distribution or reproduction in other  
forums is permitted, provided the original  
author(s) and the copyright owner(s) are  
credited and that the original publication  
in this journal is cited, in accordance with  
accepted academic practice. No use,  
distribution or reproduction is permitted  
which does not comply with these terms.

# Effect of matrix suction on the shear strength characteristics of reinforced granite residual soil

Xiangwen Deng, Zhengyu Zhu, Xi yang Lin and Xue qiang Yang\*

School of Civil and Transportation Engineering, Guangdong University of Technology, Guangzhou, China

**Introduction:** The soil in geogrid-reinforced structures is typically unsaturated, with the shear strength provided by both the matrix suction and the reinforced body. Traditional structural designs for saturated soils only consider the shear strength provided by the reinforced body, neglecting the part provided by matrix suction. As a result, the design for reinforced structures is biased toward conservatism.

**Method:** The study examined the matrix suction-provided shear strength in reinforced soils through strain-controlled triaxial and soil-water characteristic curve (SWCC) pressure plate instrumentation. The feasibility of the Schrefler and Khalili unsaturated soil shear strength formulas for predicting shear strength based on matrix suction forces was verified.

**Results:** The study revealed that the cohesion of saturated reinforced soil exhibits a significant decrease in contrast with unsaturated reinforced soil, with matrix suction serving as a crucial consideration for reinforced structure design.

**Discussion:** The experimental results confirm the suitability of applying the quasi-cohesion increment theory to reinforced clays. The Khalili formula can be utilized to predict the quasi cohesion of unsaturated reinforced soils with greater accuracy under diverse dry density conditions. The results obtained using post-shear moisture content were closer to the measured values than those using initial moisture content.

## KEYWORDS

reinforced soil, granite residual soil, matrix suction, shear strength, soil-water characteristic curve

## 1 Introduction

Granite residual soil is widely distributed in the southeast coastal area of China and is a common filling material in this area for engineering construction, and geogrid reinforced soil technology is often used to improve the overall stability of granite residual soil slopes and embankments. Based on the theory of apparent cohesion, it is well known that the reinforced geogrid mainly improves the shear strength of the soil by increasing the cohesion of the soil (Wang et al., 2021); however, the superficial layer of the filled slope is usually in the unsaturated state, and the literature (Gao et al., 2018) points out that the apparent cohesion of unsaturated granite residual soil mainly includes two parts, matrix suction and soil cohesion itself, so ignoring the influence of matrix suction on the shear strength of reinforced granite residual soil will lead to excessively cautious designs (Chehade et al., 2020).

Researchers around the world have investigated the effects of factors such as the size and shape of the reinforcing material, particle size, and loading rate on the

frictional characteristics of the interface between soil and reinforcement. They conducted these investigations using standard direct shear and pullout tests (Infante et al., 2016; Mohammadehsan and Mohammadreza, 2017; Abdi et al., 2019; Kouchaksaraei and Khalkhali, 2020; Wei-xiang et al., 2023). To investigate the stress state of reinforced soil in actual conditions, scholars both domestically and internationally have employed triaxial tests to analyze the strength and deformative properties of reinforced soil. The shear strength characteristics of reinforced soils were investigated through triaxial tests by Vidal et al. (Vidal, 1969; Lei, 2000; Zhang et al., 2023); the results of the tests revealed that the reinforcement primarily improves soil shear strength by increasing the cohesive force. Furthermore, the shear strength also varies non-linearly with an increase in the number of reinforced layers. The study by Chen et al. (Chen et al., 2014; He et al., 2019; He et al., 2021) investigated the impact of perimeter pressure, the number of reinforcement layers, and the method of reinforcement placement on the shear strength of reinforced soils using triaxial tests.

In practice, matrix suction also significantly influences the shear strength of unsaturated soils. Zhong et al. (Zhong et al., 2015) and Luo et al. (Luo and Fu, 2019) conducted triaxial testing analyses of unsaturated soil to examine the impact of matrix suction on the shear strength of unsaturated soil. The experimental results revealed that the cohesion is significantly affected by matrix suction, exhibiting a linear growth relationship. However, the effective internal friction angle is minimally influenced by matrix suction. Zhao et al. (Zhao et al., 2021) investigated the connection between soil samples' strength properties, water retention capacities, and pore sizes during cyclic direct shear testing under both wet and dry conditions. The results indicated that the decline in water retention capacities and variation in strength parameters of soil samples were primarily due to changes in pore properties. Huang et al. (Huang et al., 2022) obtained soil-water characteristic curves (SWCCs) for typical granite residual soils in Huangpu, Guangzhou, using the filter paper test method. The results indicate that the matrix suction in strongly weathered granite residual soil zones in a higher saturation state experiences smaller changes as the saturation is increased further, and maintains higher residual matrix suction than that in fully weathered granite residual soil zones. At the same time, it is suggested by much of the literature that alterations in matrix suction also impact the strength of reinforced soils. Ghazavi et al. (Bergado et al., 1993; Mahmoud and Omid, 2021) conducted a study on the impact of moisture content on peak pullout force through pullout tests. The findings indicate that there was a substantial reduction in the peak pullout force as the moisture content escalated. Zhou (Zhou and Xu, 2013) carried out consolidated undrained triaxial tests to investigate the differences in the strength characteristics of reinforced expansive soils in their saturated and unsaturated states. The results indicate that, for the same type of reinforcement, the cohesive force of the unsaturated specimen was significantly greater than that of the saturated specimen. Zhao (Zhao and Lin, 2019) derived the analytical solution for the reinforcement length needed to sustain slope stability under a linear suction distribution using the horizontal split method. The results showed that an increase in matrix suction leads to a significant decrease in the reinforcement length. At present, scholars worldwide have proposed unsaturated soil shear strength equations based on Bishop's unsaturated

shear strength equation. For instance, Cai (Guoqing et al., 2022) investigated the impact of pore ratio on the SWCC; they also introduced a novel formula to estimate the shear strength of unsaturated soils with different pore ratios and a wide range of variations in matrix suction. (Pham, 2022) proposed a shear strength equation reflecting the non-linear effects of saturation and matrix suction on the shear strength of unsaturated soils, through considering the micromechanical equilibrium conditions of the interaction among the solid, liquid, and air phases in soil. Bai (Bai et al., 2021) established a generalized principle for effective stress that can be applied to coupled processes involving heat, water, and force in both saturated and unsaturated soils, in which the approach is rooted in particle thermodynamics.

This paper is based on the municipal engineering project of the Flavor and Fragrance Industrial Park in Youxi County, Fujian Province, China, and the shear strengths and SWCC of the typical granite residual soil from Youxi were tested by using a strain-controlled triaxial instrument and SWC-150 SWCC pressure plate meter, respectively, to study the effect of matrix suctions and reinforcements on the shear strength of granite residual soil in saturated and unsaturated states, which provided certain theoretical basis and reasonable strength parameter references for actual reinforced soil structure design and construction.

## 2 Experiment

### 2.1 Reinforced geogrid and reinforced soil samples

The soil samples for testing were taken from the municipal project in Youxi County. The granite residual soil is a sandy silt with a mixture of light red and grayish-white color, slightly wet, and in a plastic to hard plastic state. The basic physical parameters of the soil measured by the indoor geotechnical tests are shown in Table 1, the particle gradation curve is shown in Figure 1A, and the static compaction curve is shown in Figure 1B.

The optimum moisture content and maximum dry density of the soil samples were measured by static compaction tests. As shown in Figure 1B, the optimum moisture content of the soil was 18.7%, and the corresponding maximum dry density was 1.73 g/cm<sup>3</sup>.

The dimensions and strength parameters of the bidirectional glass fiber geogrid used in the test are shown in Table 2, the schematic picture of the geogrid is shown in Figure 2A, and the one-layer reinforced geogrid placed in the soil sample is shown in Figure 2B.

### 2.2 Test apparatus

The conventional triaxial strain-controlled apparatus TSZ30-2.0 and volumetric pressure controller SVPC-200-3, which maintains the accuracy and stability of the pressure during the loading process, were both used together during the sample consolidation and drainage shearing process. The other accessory parts, including rubber molds, film-covering cylinders, scales, and so on, support the triaxial testing. The SWCC were measured using a SWC-150 SWCC pressure plate meter. The main instruments used in this paper are shown in Figure 3; the triaxial instrument is shown

**TABLE 1** Basic physical parameters of granite residual soil in Youxi, Fujian.

Natural moisture content (%)	Natural dry density (g/cm <sup>3</sup> )	Natural gravity (KN/m <sup>3</sup> )	Saturated gravity (KN/m <sup>3</sup> )	Plastic limit (%)	Liquid limit (%)	Plastic index
22.1	1.64	18.4	19.0	31.9	45.6	13.7

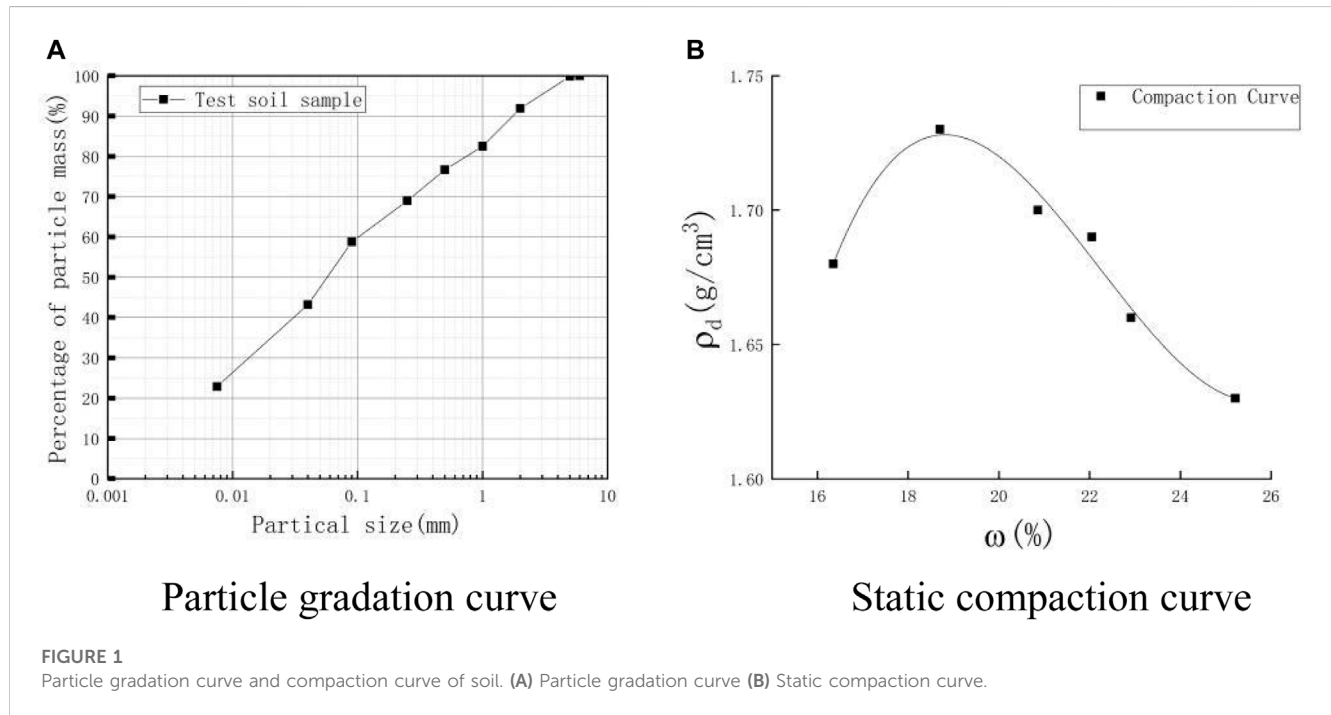


**TABLE 2** Physical parameters of the geogrid.

Name of reinforcing material	Reinforced geogrid	Mesh size (mm)	Tensile strength of glass fiber	
			Lateral (kN/m)	Longitudinal (kN/m)
Bi-directional geogrid	Glass fiber	12.7 × 12.7	50	50

in Figure 3A and the SWCC pressure plate meter is shown in Figure 3B.

### 2.3 Laboratory testing procedure

#### 2.3.1 Triaxial consolidation and drainage shear tests

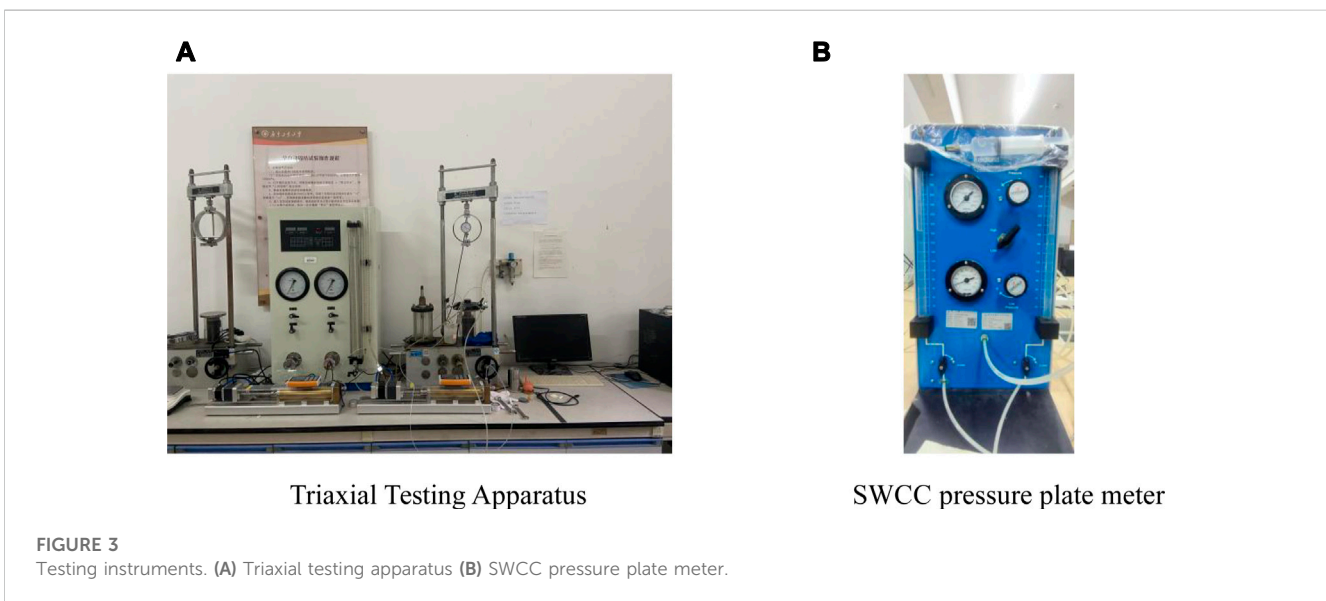
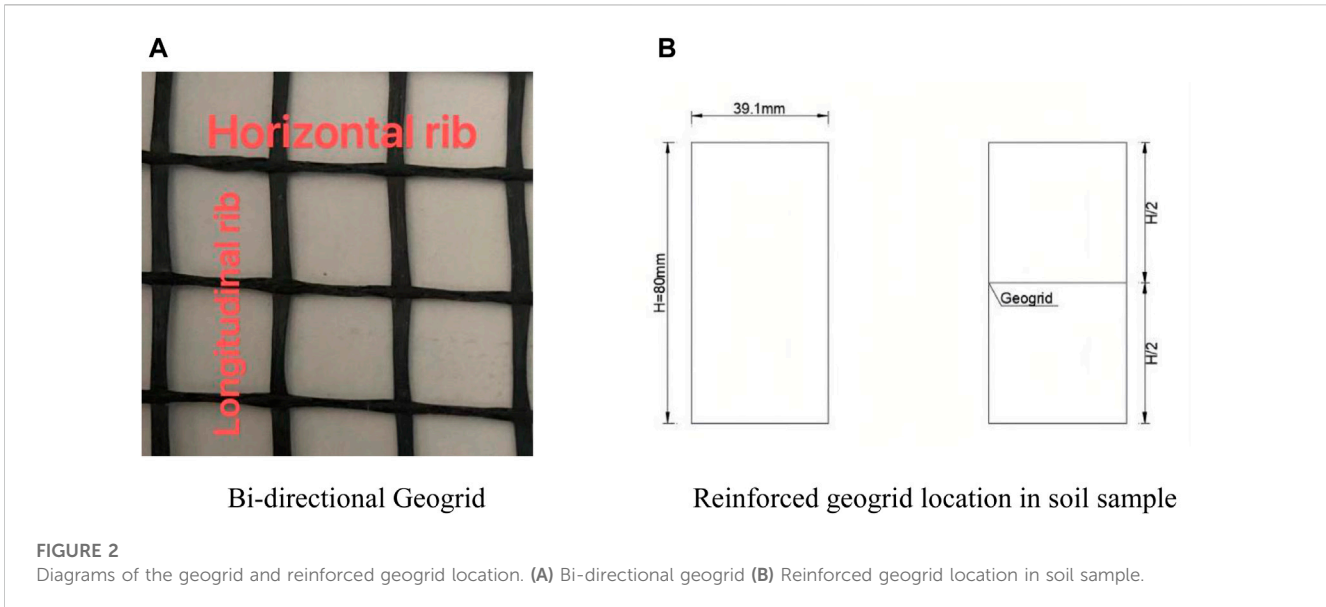
Approximately 2 kg of the residual soil was taken and then dried, crushed, and sieved through a 2 mm aperture step by step to remove the coarse particles. Finally, water was added to the remolded soil powder to reach an 18.7% moisture content and then the soil was sealed in a container for 24 h to make the moisture distribution in the soil uniform. The soil specimens with fixed dry densities and moisture content were made using the two layers static compacting soil method. After the first soil layer was compacted, the top surface of the soil layer was shaved using a scraper, and then the second layer of soil mass of the same weight was added to ensure the upper and lower layers were compacted to same compaction as far as possible.

For saturated reinforced soil specimens and saturated soil specimens, the two types of specimens were saturated using the pumping saturation method; unsaturated reinforced soil specimens were kept at a moisture content of 18.7%.

The specimen dimensions for this test were  $d = 39.1$  mm in diameter and  $h = 80$  mm in height. The triaxial consolidation and drainage shear test methodology is outlined in Table 3, wherein the unsaturated specimen displayed a water content of 18.7%.

#### 2.3.2 SWCC pressure plate meter test

In this paper, the SWC-150 SWCC pressure plate meter was used to determine the volumetric moisture contents of the residual soil under different matrix suction levels to obtain the SWCC. The soil dry density of the test was set at  $1.64$  g/cm<sup>3</sup>, and the test apparatus measures matrix suction within a range of 0 to 500 kPa. The soil specimen size was  $d = 60$  mm in diameter and  $h = 20$  mm in thickness. The testing was divided into two stages; the saturated soil specimen was put into the device for the dehydration



process firstly, and after the dehydration stage, then, water was added and absorbed until water was continued until the soil specimen became saturated again. According to the volume moisture contents and corresponding matrix suction levels obtained from the testing, SWCC could be plotted for the granite residual soil.

### 3 Test results

#### 3.1 Triaxial consolidation and drainage shearing tests

##### 3.1.1 Saturated granite residual soil tests

By rearranging the triaxial consolidation and drainage shearing test data, the stress–strain relationship curves of the saturated soil

samples under different dry densities and confining pressure levels are shown in Figure 4. It can be seen that the soil stress–strain relationship curves basically show a strain hardening tendency during the shearing process in saturated states for samples with a dry density of 1.56 g/cm<sup>3</sup>, whereas there was a slight strain softening tendency for samples with dry densities of 1.73 g/cm<sup>3</sup> and 1.64 g/cm<sup>3</sup>.

Figure 4 shows that the peak deviatoric stresses of soil specimens decrease as the dry density decreases, in which interlock friction between soil particles is lowered for the lower dry densities when shearing.

##### 3.1.2 Geogrid reinforced granite residual soil tests in saturated states

The stress–strain relationship curves of the one-layer geogrid reinforced soil samples in the consolidation shearing drainage tests

TABLE 3 Triaxial consolidation and drainage shearing test scheme.

Saturated state and number of reinforced layers		$\rho_d = 1.73 \text{ g/cm}^3$	$\rho_d = 1.64 \text{ g/cm}^3$	$\rho_d = 1.56 \text{ g/cm}^3$
Saturation state with confining pressures/kPa	Soil samples	$\sigma_3 = 100$	$\sigma_3 = 100$	$\sigma_3 = 100$
		$\sigma_3 = 200$	$\sigma_3 = 200$	$\sigma_3 = 200$
		$\sigma_3 = 300$	$\sigma_3 = 300$	$\sigma_3 = 300$
		$\sigma_3 = 400$	$\sigma_3 = 400$	$\sigma_3 = 400$
	One-layer reinforced soil samples	$\sigma_3 = 100$	$\sigma_3 = 100$	$\sigma_3 = 100$
		$\sigma_3 = 200$	$\sigma_3 = 200$	$\sigma_3 = 200$
		$\sigma_3 = 300$	$\sigma_3 = 300$	$\sigma_3 = 300$
		$\sigma_3 = 400$	$\sigma_3 = 400$	$\sigma_3 = 400$
Unsaturated state with confining pressure/kPa	One-layer reinforced soil samples	$\sigma_3 = 100$	$\sigma_3 = 100$	$\sigma_3 = 100$
		$\sigma_3 = 200$	$\sigma_3 = 200$	$\sigma_3 = 200$
		$\sigma_3 = 300$	$\sigma_3 = 300$	$\sigma_3 = 300$
		$\sigma_3 = 400$	$\sigma_3 = 400$	$\sigma_3 = 400$

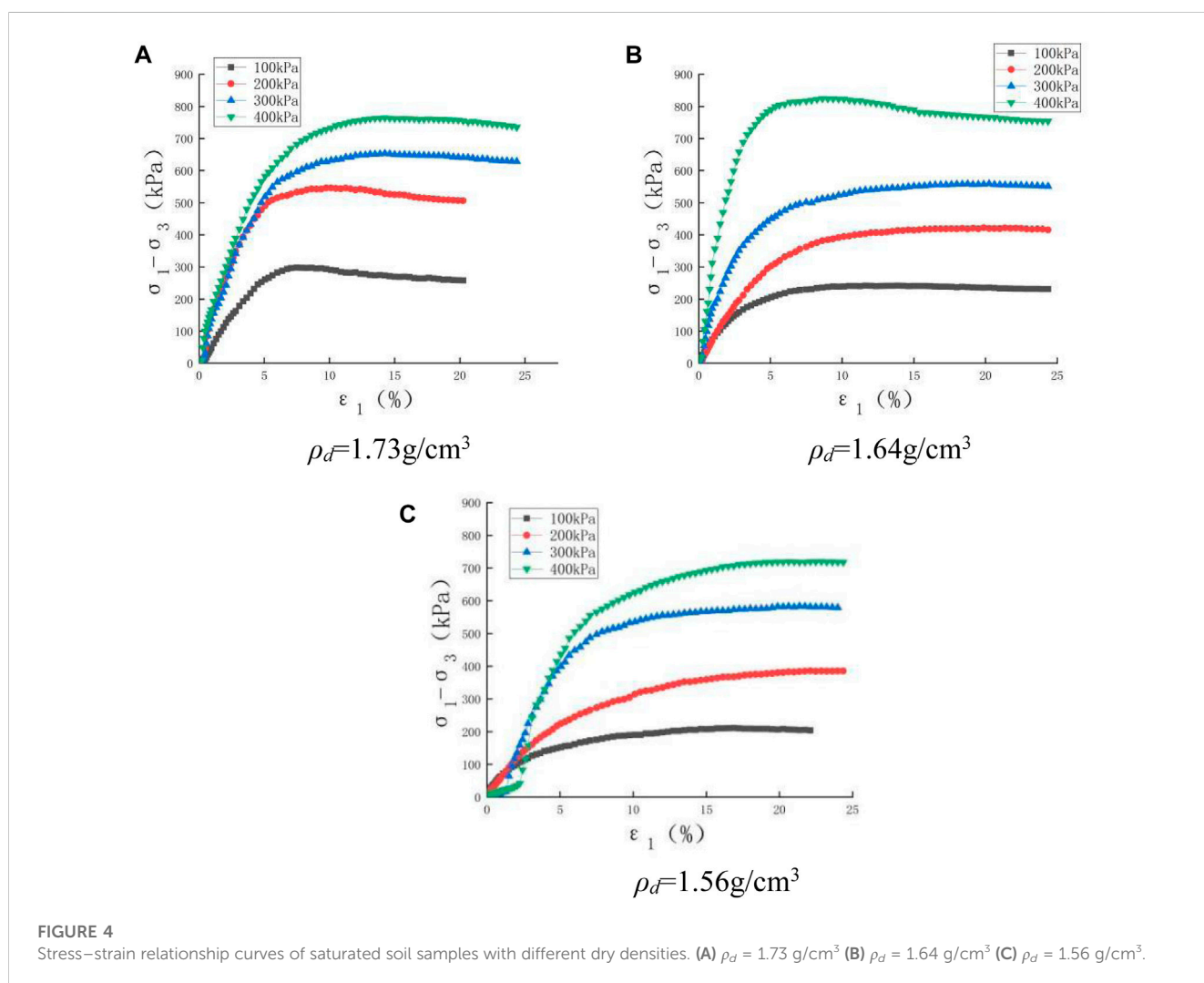
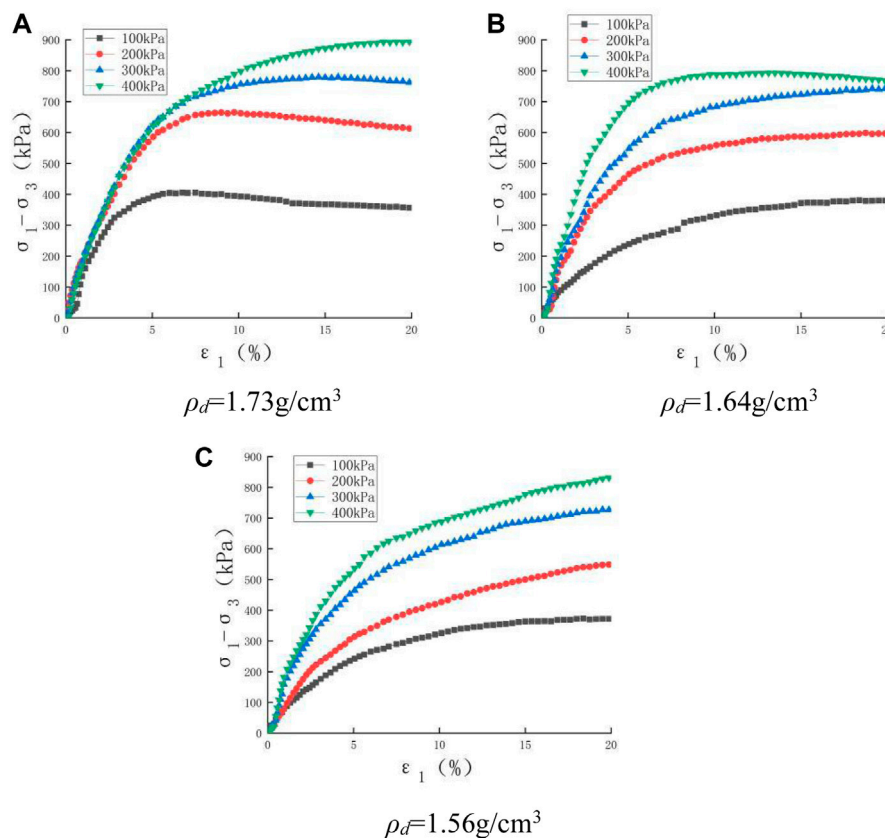


FIGURE 4 Stress-strain relationship curves of saturated soil samples with different dry densities. (A)  $\rho_d = 1.73 \text{ g/cm}^3$  (B)  $\rho_d = 1.64 \text{ g/cm}^3$  (C)  $\rho_d = 1.56 \text{ g/cm}^3$ .



**FIGURE 5**

Stress–strain relationship curves of one-layer reinforced saturated samples under consolidation drainage shear tests. (A)  $\rho_d = 1.73 \text{ g/cm}^3$  (B)  $\rho_d = 1.64 \text{ g/cm}^3$  (C)  $\rho_d = 1.56 \text{ g/cm}^3$ .

are shown in Figure 5. These basically show the trend of strain hardening, besides seldom slight strain softening curves for soil samples with a dry density of  $1.73 \text{ g/cm}^3$  under lower confining pressure levels. The peak deviatoric stresses become larger as the confining pressure and dry density were increased individually, which indicates that the peak deviatoric stresses of the reinforced specimen gradually became larger by comparing with the testing peak deviatoric stresses of unreinforced saturated soil samples as shown in Figure 4.

For one-layer geogrid reinforced soil samples in saturated states and under lower confining pressure levels such as  $\sigma_3 = 100 \text{ kPa}$ , relative horizontal displacement between the geogrid and the soil was produced obviously because of the relatively smaller frictional coefficient on the geogrid–soil interface and bigger geogrid tensile strength; this induced bulking deformation at the geogrid–soil interface location, and further soil lateral deformations along soil sample height were uneven, as shown in Figure 6A. Under higher confining pressure levels such as  $\sigma_3 = 400 \text{ kPa}$ , the relative horizontal displacement between the geogrid and the soil was still bigger, but soil lateral deformations along soil sample height were relatively even because of the higher confining pressure preventing them, as shown in Figure 6C. For the intermediate confining pressure levels such as  $\sigma_3 = 200 \text{ kPa}$ , the deformation shape of the geogrid reinforced soil samples were similar to the transition between that of Figures 6A,C.

### 3.1.3 Geogrid reinforced granite residual soil tests in unsaturated states

The one-layer geogrid reinforced specimens with three dry densities and the same moisture content of 18.7% in unsaturated states were tested in consolidation and drainage shear test, and the corresponding stress–strain curves obtained from these tests are shown in Figure 7.

From Figure 7, it can be seen that the soil particle pore space in the soil samples decreases when there is an increase in dry density, the peak deviatoric stresses of the geogrid reinforced soil increases; compared with the deviatoric stresses obtained from triaxial consolidation and the drainage shearing tests of saturated geogrid reinforced soil, the peak deviatoric stresses of unsaturated reinforced soil increased significantly due to the contribution of matrix suction.

### 3.1.4 Shear strength parameters

Based on the data from triaxial consolidation and drainage shearing tests, Table 4 summarizes the corresponding shear strength parameters.

From Table 4, it can be seen that the cohesion of the geogrid reinforced soil has a significant increase compared with that of unreinforced soil in the saturated shearing state, whereas variation in the internal friction angle was small relatively. The test results verify the correctness of the quasi-cohesion theory stated below, which is not only applicable to reinforced

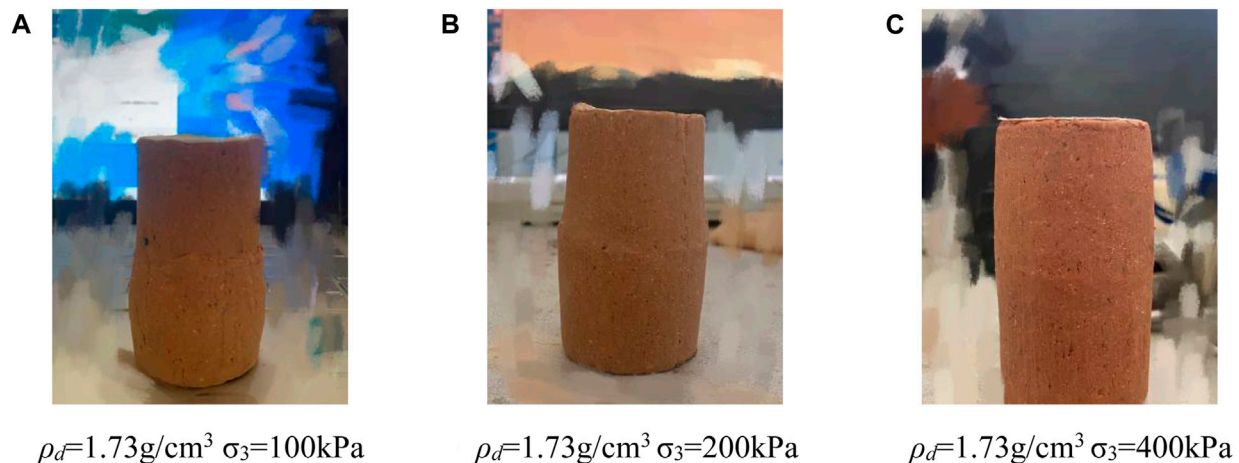


FIGURE 6

One-layer geogrid reinforced saturated sample failure status after testing. (A)  $\rho_d = 1.73 \text{ g/cm}^3$   $\sigma_3 = 100 \text{ kPa}$  (B)  $\rho_d = 1.73 \text{ g/cm}^3$   $\sigma_3 = 200 \text{ kPa}$  (C)  $\rho_d = 1.73 \text{ g/cm}^3$   $\sigma_3 = 400 \text{ kPa}$ .

sandy soil but also applicable to reinforced clay. The unsaturated geogrid reinforced soil has a significant increase in cohesion compared with that of saturated geogrid reinforced soil, which indicates that the cohesion provided by matrix suction is an important contribution that cannot be neglected totally in the design, construction, and maintenance of reinforced soil structures, and consideration of the cohesion contributed by soil matrix suction is beneficial for reinforced soil structures in reducing the construction and maintenance expense.

### 3.2 SWCC test

For the remodeled soil samples with a dry density of  $1.64 \text{ g/cm}^3$ , the SWCC between soil volume moisture contents and matrix suctions are plotted in Figure 8 using the pressure plate meter testing results.

From Figure 8, it can be seen that the SWCC in the dehydration stage differed greatly from curve in the hygroscopy stage, and there was an obvious hysteresis phenomenon between the two curves. In the process of dehydration, the volumetric moisture content gradually decreases as the matrix suction increases; whereas in the process of hygroscopy, the matrix suction gradually decreases as the volumetric moisture content in the soil increases, and the rate of change in SWCC during the hygroscopic process also transitioned from slow to fast. The appearance of the hysteresis loop reflects the unique pore size distributing pattern in the soil mass, indicating the existence of medium to large pores in dimension and uneven pore size distribution inside the soil body; the more medium to large size pores existing inside the soil body, the more water is retained in the medium to large size pores due to the bottleneck effect in the dehydration stage, which eventually leads to the increase in the hysteresis area between the dehydration curve and hygroscopy curve of the granite residual soil obtained from Youxi county.

On the other hand, the soil skeleton is deformed with the changes in volumetric moisture content in the dehydration and hygroscopy stages. In the first dehydration stage, the soil sample has

a slight decrease in pore volume induced by the increase in matrix suction due to the decrease in moisture content in the soil, and resulted in a slight decrease in the saturated volumetric water content of the soil sample was observed following the wetting stage.

## 4 Strength characteristics of geogrid reinforced soil in unsaturated states

### 4.1 Unsaturated soil shearing strength formula

Among the many shear strength formulas for unsaturated soils, Bishop's effective stress strength formula is currently the most famous. Bishop (Bishop and Blight, 1963; Xie, 2015) proposed a shear strength formula for unsaturated soils, combined with experimental studies, as expressed in Equation 1:

$$\tau = c' + [(\sigma - ua) + \chi(ua - uw)] \tan \phi' \quad (1)$$

where  $(\sigma - ua)$  denotes the net normal pressure,  $(ua - uw)$  denotes the matrix suction,  $c'$  denotes the effective cohesion, and  $\phi'$  denotes the effective internal friction angle.  $\chi$  is a parameter relating to the soil saturation and its value varies in the range of 0–1.0, which is a function of the soil saturation, soil type, and loading pressure. Since the equation is similar in form to the effective stress equation for saturated soils and relatively simple in expression, it is widely used in the study of shearing strength of unsaturated soils.

Equation 1 is further written in the form of Eq. 2:

$$\tau = c' + (\sigma - ua) \tan \phi' + \chi(ua - uw) \tan \phi' \quad (2)$$

Equation 3 can be obtained from Eq. 2 as follows:

$$c = c' + \Delta c_s = c' + \chi(ua - uw) \tan \phi' \quad (3)$$

where  $c$  is the apparent cohesion of unsaturated soil. Since the matrix suction is associated with the soil moisture content and  $\Delta c_s$  is the quasi-cohesion increment induced by the matrix suction, scholars

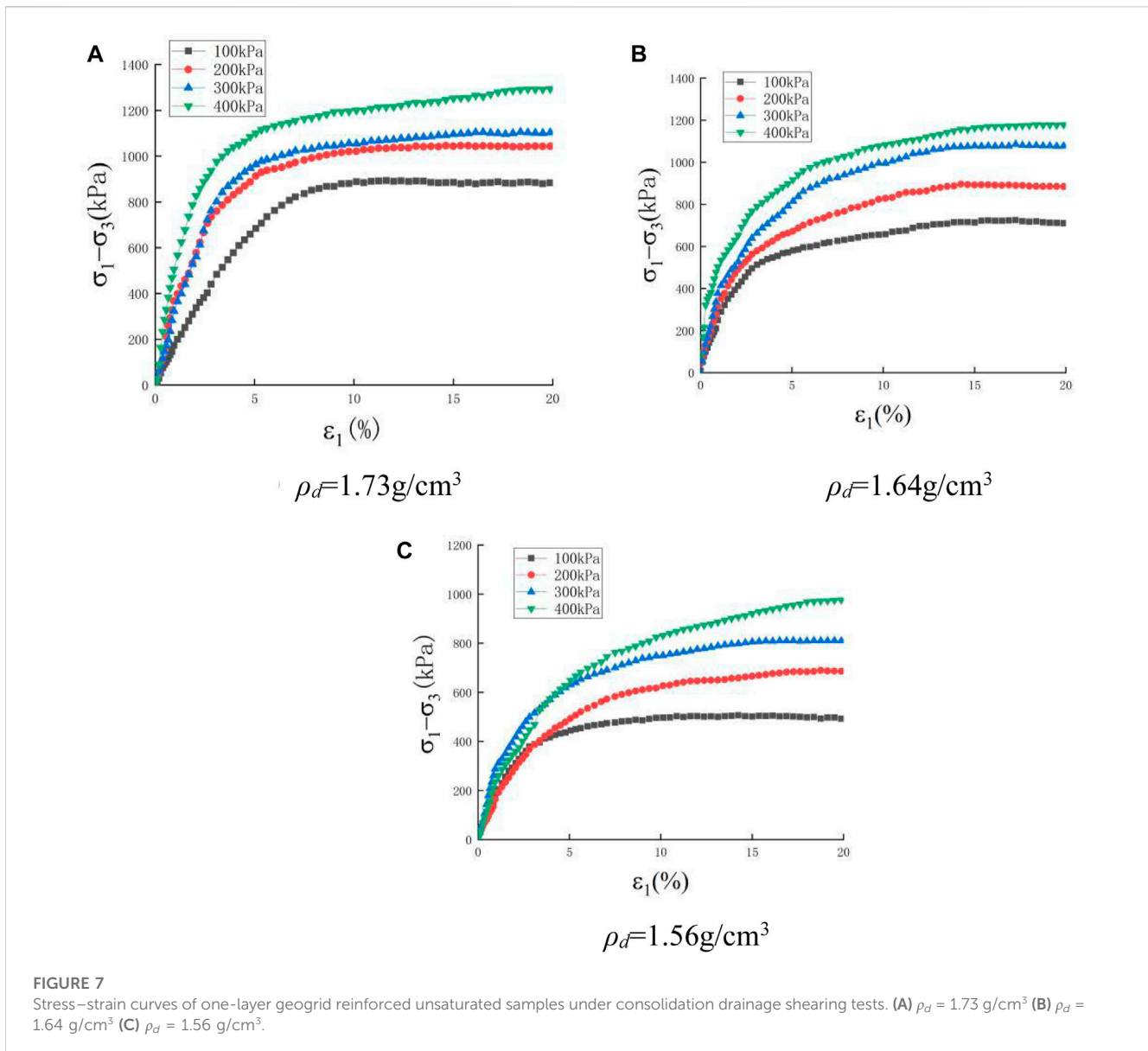


**TABLE 4** Shearing strength parameters under triaxial consolidation drainage.

Dry density/(g/cm <sup>3</sup> )	1.73	1.64	1.56
Saturated unreinforced soil	$c' = 37.57 \text{ kPa}$	$c' = 24.10 \text{ kPa}$	$c' = 12.14 \text{ kPa}$
	$\phi' = 24.7^\circ$	$\phi' = 24.1^\circ$	$\phi' = 22.3^\circ$
Saturated geogrid reinforced soil	$c = 74.74 \text{ kPa}$	$c = 68.36 \text{ kPa}$	$c = 59.63 \text{ kPa}$
	$\phi' = 26.4^\circ$	$\phi' = 28.2^\circ$	$\phi' = 25.5^\circ$
Unsaturated geogrid reinforced soil	$c = 243.37 \text{ kPa}$	$c = 189.96 \text{ kPa}$	$c = 148.37 \text{ kPa}$
	$\phi' = 27.7^\circ$	$\phi' = 27.8^\circ$	$\phi' = 27.3^\circ$

established the parameter  $\chi$  as a function of volume water content or saturation based on the SWCC to avoid the complicating experimental measurements.

Schrefler (Schrefler, 1984) proposed soil saturation replacing  $\chi$  to derive Eq. 4 for the shearing strength of unsaturated soils:



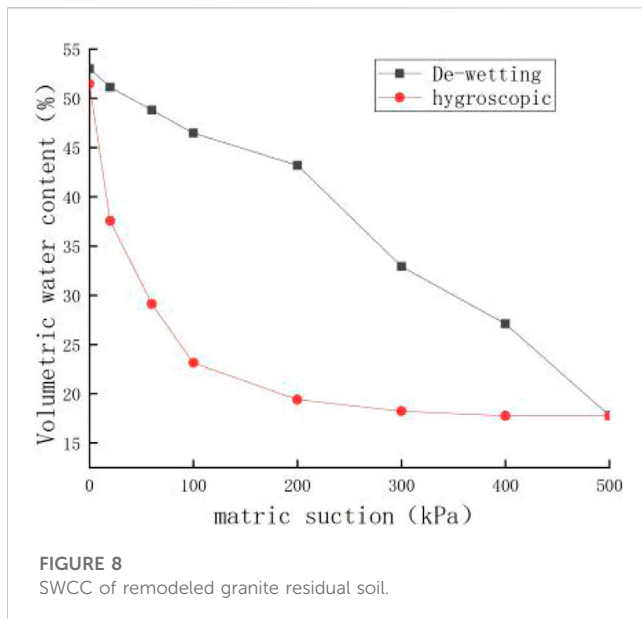


FIGURE 8 SWCC of remodeled granite residual soil.

$$\tau_f = c' + (ua - uw)Sr \tan \phi' + (\sigma - ua) \tan \phi' \quad (4)$$

Khalili et al. (Khalili and Khabbaz, 1998) introduced an air-entry suction value of unsaturated soil through extensive experimental studies and proposed the unsaturated soil shearing strength Eq. 5 as follows:

$$\tau_f = c' + (ua - uw) \left[ \frac{ua - uw}{(ua - uw)b} \right]^{-0.55} \tan \phi' + (\sigma - ua) \tan \phi' \quad (5)$$

where  $(ua - uw)b$  is the air-entry suction of unsaturated soil; this replaces the Eq. 3 parameter  $\chi$  as the form  $[(ua - uw)/(ua - uw)b]^{-0.55}$  to improve Bishop's formula shearing strength prediction ability for the unsaturated soil.

## 4.2 Quasi-cohesion increment calculation

The current research focuses on the reinforcement strengthening mechanism in reinforced soil as well as the corresponding equivalent quasi-cohesion increment calculating method. The quasi-cohesion increment calculation considers the internal friction angle of reinforced soil being basically equal to that of unreinforced soil, reinforcement simply increases the cohesion of the soil mass.

The quasi-cohesion increment calculation of reinforced soil could be explained further by using Mohr–Coulomb failure criterion as Eq. 6 expressing:

$$\sigma_{1f} = \sigma_3 \tan^2 \left( 45^\circ + \frac{\phi'}{2} \right) + 2(c' + \Delta c_r) \tan \left( 45^\circ + \frac{\phi'}{2} \right) \quad (6)$$

where  $\sigma_{1f}$  represents the major principal stress, kPa, at the shearing failure state of the reinforced soil;  $\sigma_3$  represents the minor principal stress, kPa;  $c'$  represents soil effective cohesion, kPa;  $\phi'$  represents angle of effective internal friction, °; and  $\Delta c_r$  is the quasi-cohesion increment contributed by the geogrid reinforcing function, kPa.

Comparing Eq. 6 with the limit equilibrium condition of unreinforced soil, the quasi-cohesion increment  $\Delta c_r$  contributed by the geogrid reinforced function in the reinforced soil can be calculated.

Through the triaxial compression tests of reinforced soil, the action of the reinforced geogrid in the soil can be regarded as an additional equivalent minor stress increment acting on the soil mass, thus the  $\Delta c_r$  formula (7) is proposed as follows:

$$\Delta c_r = \frac{\Delta \sigma_3 \tan \left( 45^\circ + \frac{\phi'}{2} \right)}{2} \quad (7)$$

where  $\Delta \sigma_3$  is the equivalent minor principal stress increment, generated by the reinforced geogrid restriction, and the increment cannot be measured directly and can be predicted theoretically. Eqs. 8 and 9 can be obtained from Figure 9 as follows:

$$\sigma_{1f} = \sigma_{3f} k_p + 2c'(k_p)^{1/2} \quad (8)$$

$$\sigma_1 = \sigma_3 k_p + 2c'(k_p)^{1/2} \quad (9)$$

Subtracting Eq. 8 from Eq. 9, then Eq. 10 is obtained:

$$k_p = \frac{\sigma_{1f} - \sigma_1}{\sigma_{3f} - \sigma_3} = \frac{\Delta \sigma_1}{\Delta \sigma_3} \quad (10)$$

Substituting Eq. 10 into Eq. 9, then Eq. 11 is obtained:

$$\Delta \sigma_3 = \sigma_3 \left[ \frac{\Delta \sigma_1}{\sigma_1 - 2c'(k_p)^{1/2}} \right] \quad (11)$$

Substituting Eq. 11 into Eq. 7, the quasi-cohesion increment of reinforced soil can be deduced as Eq. 12:

$$\Delta c_r = \frac{\sigma_3 \sqrt{k_p}}{2} \left( \frac{\Delta \sigma_1}{\sigma_1 - 2c' \sqrt{k_p}} \right) \quad (12)$$

The quasi-cohesion increments of reinforced soil are calculated from Eq. 12, and are further compared with the measuring cohesion increments, as shown in Table 5.

As shown in Table 5, the increase in quasi-cohesion increments calculated by Eq. 12 is smaller than the measured value, which is because Eq. 12 calculates the quasi-cohesion increments only by the peak stress difference and the effective cohesion and effective angle of internal friction of the unreinforced soil, and does not sufficiently consider the influence of the reinforcing material, the size of the reinforcing material, and the number of reinforcing layers, which results in the calculated value usually being smaller than the measured value. The quasi-cohesion increments calculated based on the theory of quasi-cohesion for the reinforcing body shows a slight discrepancy from the measured value obtained from testing. However, the difference is relatively small and can be utilized as the safety consideration for reinforced soil structures.

## 4.3 Calculation of the shearing strength of unsaturated reinforced soil

It is usually difficult to measure the volumetric moisture content of the specimen during the shearing process; thus, this limits the study of shearing strength characteristics of the

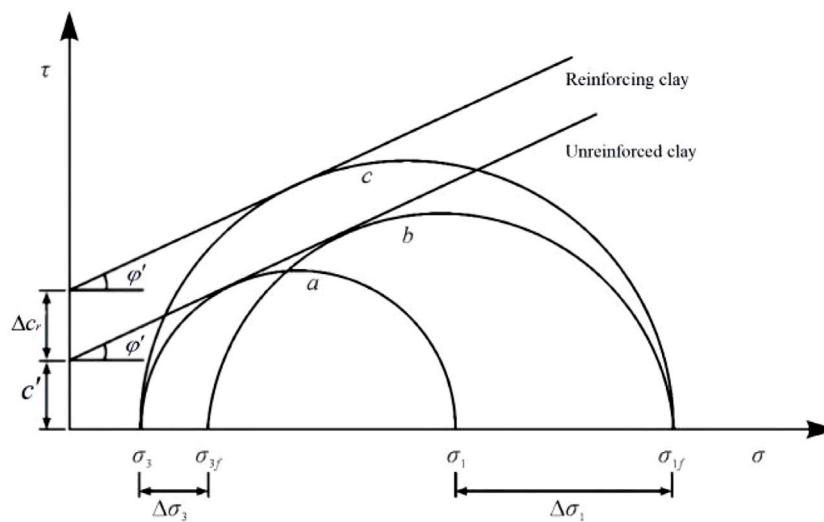


**FIGURE 9**  
Stress analyses of reinforced and unreinforced clay samples.

**TABLE 5** Calculating and measuring increments of quasi-cohesion of saturated reinforced clay.

Dry density/ (g/cm <sup>3</sup> )	Confining pressure/kPa	Peak deviatoric stress of reinforced soil/kPa	Peak deviatoric stress of unreinforced soil/kPa	Peak deviatoric stress difference/kPa	Quasi-cohesion increment Δc <sub>r</sub> /kPa	Measuring quasi-cohesion increment/kPa
1.73	100	392.8	284.2	108.6	31.40	37.14
	200	662.1	545.9	116.2		
	300	756.4	627.0	129.4		
	400	798.4	724.8	73.6		
1.64	100	332.4	239.2	93.2	41.28	44.26
	200	559.3	394.5	164.8		
	300	683.4	526.1	157.3		
	400	787.2	699.8	87.4		
1.56	100	325.8	180.1	145.7	39.62	47.49
	200	426.1	313.6	112.5		
	300	613.8	501.7	112.1		
	400	688.0	585.5	102.5		

unsaturated soil to some extent, because the volumetric moisture content of the specimen at shearing failure is easily measured, usually to be used to evaluate shear strength of unsaturated soil, as pointed out in the literature (Zhao, 2022). It can be also assumed approximately that the volume change of the specimen during shear is small, and the volumetric moisture content during shear is close to the initial volumetric moisture content. Based on the moisture absorbing curve in Figure 8, the shearing strengths of unsaturated reinforced soil are calculated in this section using the shearing failure volumetric water content and initial volumetric water content separately,

and the calculating shear strengths using the two volumetric water contents are compared and commented upon further.

The volume moisture contents of unsaturated reinforced granite residual soil on shearing failure for the triaxial CD tests were measured, and corresponding matrix suctions are shown in Table 6. As can be seen from Table 6, there is a slight increase in the moisture content of the specimens after shearing compared with the initial moisture content of 18.7%.

- 1) Schrefler's formula for shear strength of unsaturated reinforced soil

TABLE 6 Water contents of specimens after shearing and the corresponding matrix suctions.

Dry density/(g/cm <sup>3</sup> )	Confining pressure/kPa	Volume moisture content after shearing/%	Saturation/%	Matrix suction/kPa
1.73	100	19.9	42.2	251.75
	200	21.1	44.7	208.70
	300	20.8	44.1	218.71
	400	21.7	46.0	189.69
1.64	100	20.0	37.8	245.74
	200	22.0	41.5	180.68
	300	18.9	35.7	295.29
	400	19.6	37.0	263.76
1.56	100	20.7	35.0	222.22
	200	19.8	33.2	255.75
	300	20.3	34.1	236.23
	400	21.4	35.9	198.69

The saturation in Table 6 can be substituted into Eq. 3 to calculate the quasi-cohesion increment of unsaturated reinforced granite residual soil, and the calculated results are summarized in Figure 10. The calculated results have obvious differences with the experimental measured values, which are due to the fact that the shear strength formula proposed by Schrefler only considers the linear effect of saturation on shear strength, thus Schrefler's formula cannot better reflect the effect of matrix suction on the shearing strength of unsaturated soil correctly.

2) Khalili unsaturated soil shear strength formula

From the literature (Zhang, 2018) and the testing results in this paper, it is known that the air-entry matrix suction of granite residual soil is about 10 kPa, thus  $(u_a - u_w)b = 10\text{kPa}$  is used for calculation so that the apparent cohesion of unsaturated reinforced granite residual soil can be calculated by substituting the air-entry matrix suction 10 kPa into Equation 5, and the calculating results are summarized in Figure 10.

At the same time, the cohesion of unsaturated reinforced granite residual soil was also calculated using the initial volume moisture content 18.7% of the specimen, and corresponding matrix suction of granite residual soil according to initial volume moisture content 18.7% was read as 279.27 kPa from the moisture absorbing curve in Figure 8, and the apparent cohesion of the unsaturated reinforced granite residual soil was calculated according to Eq. 13. The calculated results were also shown in Figure 10:

$$c = c' + \Delta c_r + \Delta c_s = c' + \frac{\sigma_3 \sqrt{k_p}}{2} \left( \frac{\Delta \sigma_1}{\sigma_1 - 2c' \sqrt{k_p}} \right) + \chi (u_a - u_w) \tan \phi' \tag{13}$$

where  $\Delta c_s$  is the apparent cohesion increment induced by matrix suction, being different from quasi-cohesion increment  $\Delta c_r$ , contributed by the geogrid restriction.

As shown in Figure 10, relatively to the Schrefler unsaturated soil shear strength formula, the Khalili unsaturated soil shear strength formula can predict the cohesion of unsaturated reinforced soil more accurately, in

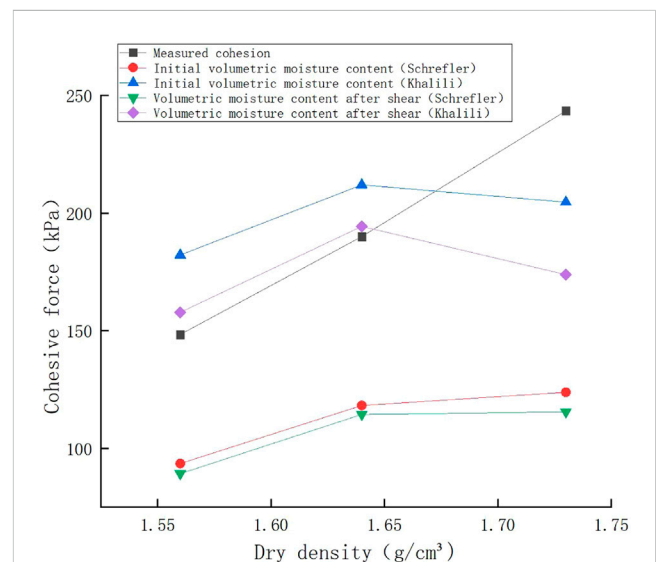
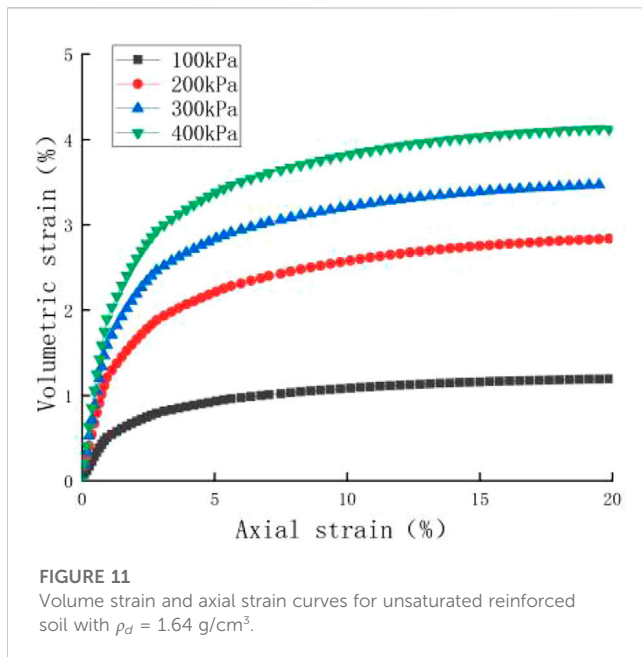


FIGURE 10 Calculated and measured cohesions of unsaturated reinforced granite residual soil.

which the cohesion includes three parts, i.e., effective cohesion  $c'$  contributed by the soil mass itself, apparent cohesion increment  $\Delta c_s$  produced by matrix suction, and quasi-cohesion increment  $\Delta c_r$  contributed by reinforced effecting of geogrid. Comparing the cohesion calculated using the shearing failure volume moisture content with cohesion calculated based on initial volume moisture content, the cohesion calculated using the shearing failure volume moisture content is closer to the measured cohesion of the unsaturated reinforced soil. The calculating cohesion errors using the Khalili method were 2.28% for the dry density 1.64 g/cm<sup>3</sup> sample and 6.36% for the dry density 1.56 g/cm<sup>3</sup> sample, and calculating cohesion for the dry density 1.73 g/cm<sup>3</sup> sample can also reflects the measured value to some extent, but the error is large.



When the initial volume moisture content was considered, the errors using the Khalili method were significantly larger for the dry density  $1.64 \text{ g/cm}^3$  and  $1.56 \text{ g/cm}^3$  samples than those calculated using the shearing failure volume moisture content, but the error for the dry density  $1.73 \text{ g/cm}^3$  sample was relatively smaller.

Combining SWCC under a specific dry density condition with the Khalili formula may predict the cohesion of unsaturated reinforced soil approaching the specific dry density for unsaturated soil. Thus, formula (13) provides theoretical and experimental evidence to support the practical design, construction, and maintenance of reinforced soil structures.

It is also important to add in that both unsaturated soil and unsaturated reinforced soil tests always keep the back pressure at zero during testing, as the water content in soil samples do not have enough time to change during the triaxial shear process, and the volume change of unsaturated reinforced soil is caused mainly due to gas seepage; thus, soil volume at the moment of shearing failure is expressed in Eq. 14:

$$v = (1 - \varepsilon_{vf})v_0, \varepsilon_{vf} = \varepsilon_{1f} + 2\varepsilon_{3f} \quad (14)$$

In order to verify the volume change mainly induced by gas seepage, a smaller back pressure of 20 kPa was applied for the soil specimen triaxial consolidation and drainage shear test in unsaturated states. During the shear test, any gas or water discharged from the specimen was measured. To minimize the impact of back pressure on the results, a lower back pressure 20 kPa was used. Using the dry density  $1.64 \text{ g/cm}^3$  specimens for the tests, Figure 11 displays the volume strain curves acquired through the triaxial consolidation and drainage shear tests.

The volumetric water contents calculated from Eq. 14 at the moment of shearing failure approached the measured values listed in

Table 6, which indicates that the volume change was mainly due to dissipated gas.

## 5 Conclusion

- 1) Unsaturated reinforced soil has a significantly greater cohesion than saturated reinforced soil due to matrix suction. Experimental and theoretical results indicate that matrix suction contributes more to the total cohesion.
- 2) The water-added remodeling process of granite residual soil exhibited similarities to the hygroscopic stage. As a result, utilizing the hygroscopic stage's soil-water characteristic curve allows for more accurate prediction of the apparent cohesion increment of unsaturated soil.
- 3) Quasi-cohesion increment calculating using formula (12) for the geogrid reinforced saturated soil was verified to be correct compared with the experimental results; Khalili's modified formula accurately predicts the quasi-cohesive strength of unsaturated reinforced soils based on the effective cohesion, matrix suction, and reinforcement, as demonstrated.
- 4) By verifying theoretical results to the results of triaxial tests with three dry density specimens in unsaturated states, it is pointed that the Khalili unsaturated soil shear strength formula predicts the shear strength of soil using shearing failure volumetric water content slightly better than that calculated using the initial volumetric water content, by using reasonable SWCC.

## Data availability statement

The raw data supporting the conclusion of this article will be made available by the authors, without undue reservation.

## Author contributions

XD: Writing—original draft. ZZ: Writing—original draft. XL: Writing—original draft. XY: Writing—review and editing.

## Funding

The author(s) declare financial support was received for the research, authorship, and/or publication of this article. National Natural Science Foundation of China (51978177).

## Conflict of interest

The authors declare that the research was conducted in the absence of any commercial or financial relationships that could be construed as a potential conflict of interest.

## Publisher's note

All claims expressed in this article are solely those of the authors and do not necessarily represent those of their affiliated

organizations, or those of the publisher, the editors and the reviewers. Any product that may be evaluated in this article, or claim that may be made by its manufacturer, is not guaranteed or endorsed by the publisher.

## References

- Abdi, M. R., Zandieh, A. R., Mirzaefar, H., and Arjomand, M. A. (2019). Influence of geogrid type and coarse grain size on pull out behaviour of clays reinforced with geogrids embedded in thin granular layers. *Eur. J. Environ. Civ. Eng.* 25 (12), 2161–2180. doi:10.1080/19648189.2019.1619627
- Bai, B., Zhou, R., Cai, G., Hu, W., and Yang, G. (2021). Coupled thermo-hydro-mechanical mechanism in view of the soil particle rearrangement of granular thermodynamics. *Comput. Geotechnics* 137 (8), 104272. doi:10.1016/j.compgeo.2021.104272
- Bergado, T. D., Shivashankar, R., Alfaro, C. M., Chai, J. C., and Balasubramaniam, A. S. (1993). Interaction behaviour of steel grid reinforcements in a clayey sand. *Géotechnique* 43 (4), 589–603. doi:10.1680/geot.1993.43.4.589
- Bishop, A. W., and Blight, G. E. (1963). Some aspects of effective stress in saturated and partly saturated soils. *Géotechnique* 13 (3), 177–197. doi:10.1680/geot.1963.13.3.177
- Chehade, A. H., Dias, D., Sadek, M., Jenck, O., and Hage Chehade, F. (2020). Upper bound seismic limit analysis of geosynthetic-reinforced unsaturated soil walls. *Geotext. Geomembranes* 48 (4), 419–430. doi:10.1016/j.geotextmem.2020.02.001
- Gao, Y., Chang, L. I. U., Tian, W., and Zhao, Y. (2018). Experimental study on the relationship between saturation and shear strength of silty clay. *Pearl River* 39 (02), 1–4.
- Guoqing, C., Yi, L., Jian, L., Yang, R., and Zhao, C. (2022). Water retention curve with different void ratios over a wide suction range and its application to shear strength. *Int. J. Geomechanics* 22 (8). doi:10.1061/(asce)gm.1943-5622.0002484
- He, Y., Liao, H., and Dong, Q. (2021). Experimental study on strength characteristics of geogrid-reinforced loess. *Chin. J. Geotechnical Eng.* 43 (S1), 181–185. doi:10.11779/CJGE2021S1033
- He, Z. J., SiGa, A., and Zou, J. F. (2019). Research for reinforced fine-grained sand based on large-scale triaxial tests. *J. Railw. Sci. Eng.* 16 (10), 2451–2458. doi:10.19713/j.cnki.43-1423/u.2019.10.010
- Huang, J., Fan, P., and Shan, Y. (2022). Study on unsaturated characteristics of granite residual soil and its slope stability. *Build. Struct.* 52 (24), 138–143. doi:10.19701/j.jzjz.20220082
- Infante, U. J. D., Martinez, A. M. G., Arrua, A. P., and Eberhardt, M. (2016). Shear strength behavior of different geosynthetic reinforced soil structure from direct shear test. *Int. J. Geosynth. Ground Eng.* 2 (2), 17. doi:10.1007/s40891-016-0058-2
- Khalili, N., and Khabbaz, M. H. (1998). A unique relationship for  $\chi$  for the determination of the shear strength of unsaturated soils. *Geotechnique* 48 (5), 681–687. doi:10.1680/geot.1998.48.5.681
- Kouchaksaraei, K. M., and Khalkhali, B. A. (2020). The effect of geocell dimensions and layout on the strength properties of reinforced soil. *SN Appl. Sci.* 2 (10), 1701. doi:10.1007/s42452-020-03480-w
- Lei, S. Y. (2000). Study on reinforced loess by triaxial tests. *J. Xi'an Highw. Univ.* (02), 1–5. doi:10.3321/j.issn:1671-8879.2000.02.001
- Luo, X., and Fu, M. (2019). Experimental study of strength characteristics of unsaturated granite residual soil in collapsing erosion area. *Water Power* 45 (01), 107–111. doi:10.3969/j.issn.0559-9342.2019.01.027
- Mahmoud, G., and Omid, B. (2021). Analytical solution for calculation of pull out force-deformation of geosynthetics reinforcing unsaturated soils. *Geotext. Geomembranes*. doi:10.1016/j.geotextmem.2021.12.005
- Mohammadehsan, Z., and Mohammadreza, Z. (2017). Study on the impact of strain rate and loading speed on geogrid-reinforced soil. *J. Sustain. Dev.* 10 (2), 238. doi:10.5539/jsd.v10n2p238
- Pham, A. T. (2022). Micromechanical-Based Shear strength equation considering the stress-state effect for unsaturated soils. *Int. J. Geomechanics* 22 (9). doi:10.1061/(ASCE)GM.1943-5622.0002495
- Schrefler, B. A. (1984). *The finite element method in soil consolidation:with applications to surface sidence*. Swansea: University College of Swansea.
- Vidal, H. (1969). *The principle of reinforced earth*. Washington, D.C.: Highway Research Record.
- Wang, Z., Chang, L. I., and Xiao, L. (2021). Triaxial test study on reinforcement effect of reinforced cohesive soil. *J. Chongqing Jiaot. Univ. Nat. Sci.* 40 (07), 99–106. doi:10.3969/j.issn.1674-0696.2021.07.15
- Wei-xiang, Z., Meng-jie, Y., and Fei-yu, L. (2023). Investigation on the cyclic shear response of stereoscopic geogrid-reinforced coarse-grained soil interface. *Transp. Geotech.* 38. doi:10.1016/j.trgeo.2022.100905
- Chen, X., Zhang, J., and Li, Z. (2014). Shear behaviour of a geogrid-reinforced coarse-grained soil based on large-scale triaxial tests. *Geotext. Geomembranes* 42 (4), 312–328. doi:10.1016/j.geotextmem.2014.05.004
- Xie, D. (2015). *Soil mechanics for unsaturated soils*. Beijing: Higher Education Press.
- Zhang, He, and YaLong, L. I. (2023). Study of mechanical properties of reinforced red sandstone. *J. Liaoning Tech. Univ. Sci.* 42 (02), 143–151. doi:10.11956/j.issn.1008-0562.2023.02.003
- Zhang, S. (2018). *The safety of the unsaturated soil slope stability analysis under different moisture content*. Shijiazhuang, China: Shijiazhuang Tiedao University.
- Zhao, B., and Lin, Y. (2019). Stability analysis of the reinforced soil retaining wall against unsaturated soils. *Railw. Eng.* 59 (10), 100–103. doi:10.3969/j.issn.1003-1995.2019.10.24
- Zhao, J., Xu, Z., and Chai, J. (2021). Experimental investigation in strength and water retention behaviors of remolded loess under drying-wetting cycle. *Water Resour. Power* 39 (09), 169–172+139.
- Zhao, L. (2022). *Research on physical and mechanical properties of unsaturated soil for Lanzhou-Cooperative high-speed railway line*. Xi'an, China: Chang'an University.
- Zhong, Z., Liu, Y., Liu, X., Li, X. y., and Wang, S. (2015). Influence of moisture content on shearing strength of unsaturated undisturbed quaternary system middle pleistocene. *J. Central South Univ.* 22 (7), 2776–2782. doi:10.1007/s11771-015-2808-z
- Zhou, J., and Xu, H. (2013). Triaxial tests of expansive soil reinforced with basalt fiber geogrid. *J. Nanjing Univ. Technol. Nat. Sci. Ed.* 35 (05), 105–109. doi:10.3969/j.issn.1671-7627.2013.05.020